Diagnosing the Factors That Contribute to the Intermodel Spread of Climate Feedback in CMIP6

CHENGGONG WANG,[a] WENCHANG YANG,[b] GABRIEL VECCHI,[a,b,c] BOSONG ZHANG,[a] BRIAN J. SODEN,[d] AND DUO CHAN[e]

[a] *Program in Atmospheric and Oceanic Sciences, Princeton University, Princeton, New Jersey*
[b] *Department of Geosciences, Princeton University, Princeton, New Jersey*
[c] *High Meadows Environmental Institute, Princeton University, Princeton, New Jersey*
[d] *Rosenstiel School of Marine and Atmospheric Sciences, University of Miami, Miami, Florida*
[e] *Department of Physical Oceanography, Woods Hole Oceanographic Institution, Woods Hole, Massachusetts*

(Manuscript received 5 September 2023, in final form 3 October 2024, accepted 19 November 2024)

ABSTRACT: The global surface temperature climate feedback parameter λ varies significantly across climate models, and its real-world value remains uncertain. Studies have found that the sea surface temperature (SST) response pattern and atmospheric model physics can each affect the climate feedback parameter in historical and idealized warming simulations. In this study, we design and analyze a series of the targeted atmospheric global climate model (AGCM) experiments to quantify how much the SST (both the warming pattern and the base climatology) and atmospheric model physics contributes to the intermodel spread of the climate feedback parameter and cloud feedback in phase 6 of the Coupled Model Intercomparison Project (CMIP6). We use three AGCMs, HiRAM, AM2.5, and AM4, developed in the Geophysical Fluid Dynamics Laboratory (GFDL), which span a wide range of feedbacks in response to uniform surface warming. The three GFDL models indicate that historical patterns of SST change systematically alter λ, supporting the hypothesized role for a "pattern effect" in historical climate sensitivity. However, we found that forcing one AGCM with the different CO_2-induced SST warming patterns or model SST climatology from a suite of climate models from CMIP6 can only reproduce ~10% the intermodel spread of CO_2-induced λ, while the atmospheric model used determines the magnitude of λ (~45%). This underscores the role of atmospheric model physics in altering λ, particularly the cloud-related schemes. In addition, we demonstrate that the nonlinear interaction between SST and AGCM has a nonnegligible role in affecting λ.

KEYWORDS: Sea surface temperature; Climate models; Coupled models; Model comparison; Model evaluation/performance

1. Introduction

The global surface temperature climate feedback parameter λ quantifies the efficiency with which the climate system restores the radiative equilibrium in response to an external forcing. The inverse of the feedback parameter reflects the global surface temperature climate sensitivity: how much Earth needs to warm or cool to balance one unit of change in radiative forcing. As the climate science community continues efforts to better understand and narrow uncertainties in climate feedback/sensitivity (Sherwood et al. 2020; Caldwell et al. 2018; Manabe and Wetherald 1967; Cess et al. 1990; Forster et al. 2023), past and the current generations of climate models (GCMs) still exhibit a significant range in climate feedback/sensitivity, which is primarily due to uncertainties in the cloud feedback (Zelinka et al. 2020; Soden et al. 2008; Wang et al. 2021; Andrews et al. 2012; Caldwell et al. 2016). Understanding the contributing factors behind the intermodel spread in λ may help to narrow down the uncertainty in climate sensitivity and help direct efforts of model development, theory, and observations.

Poor constraints on the parameterization of convection and other cloud-related schemes within the atmospheric component of GCMs (AGCM) have been suggested to be the dominant source of intermodel spread in cloud feedback (Sanderson et al. 2008; Zhao 2014). Different treatments of cumulus precipitation efficiency within the same model can yield different cloud feedback and climate feedback parameters (Zhao et al. 2016; Mülmenstädt et al. 2021; Bjordal et al. 2020). Previous studies also showed that the treatment of supercooled liquid water can significantly impact the shortwave cloud feedback over the Southern Ocean and the climate sensitivity (Zelinka et al. 2020; Bjordal et al. 2020; McCoy et al. 2014, 2015; Tan et al. 2016; Ceppi et al. 2016). By examining the correlation between the amip-p4K and abrupt-4xCO2 climate feedback parameters, Qin et al. (2022) found that around half of the intermodel spread in climate feedback across the coupled GCMs can be attributed to the corresponding atmospheric-only simulations in phase 5 and phase 6 of the Coupled Model Intercomparison Project (CMIP5 and CMIP6). Similar correlations are also found between the amip-piForcing and abrupt-4xCO2 climate feedback parameters (Andrews et al. 2022, 2018).

In addition to atmospheric model physics, it has been found that the sea surface temperature (SST) warming pattern can strongly regulate λ. The climate feedback parameter in a

Denotes content that is immediately available upon publication as open access.

Supplemental information related to this paper is available at the Journals Online website: https://doi.org/10.1175/JCLI-D-23-0528.s1.

Corresponding author: Chenggong Wang, c.wang@princeton.edu

DOI: 10.1175/JCLI-D-23-0528.1

GCM is not a constant value, rather it changes with evolving warming patterns (Armour et al. 2013; Winton et al. 2010; Andrews et al. 2015; Dong et al. 2019, 2020). This is particularly important during the last several decades where the observed warming in the Pacific differs markedly from coupled model predictions. Many studies indicate that the observed pattern of warming generates a more negative cloud feedback than the coupled model simulate with either historical or idealized 4xCO2 forcings (Zhou et al. 2016; Fueglistaler and Silvers 2021; Andrews et al. 2022). Tropical convected regions, like the western Pacific warm pool, have strong nonlocal effect and effectively modify the top of atmosphere fluxes due to weak gradient temperature (Zhou et al. 2017; Dong et al. 2019; Zhang et al. 2023; Williams et al. 2023; Bloch-Johnson et al. 2024). However, it is important to note that the climate models rarely capture the observed warming pattern, warming in the Indo-Pacific warm pool and slight cooling in the eastern equatorial Pacific, in the past decades (Wills et al. 2022; Seager et al. 2022; Fueglistaler and Silvers 2021). It remains an open question that whether this is due to lack of variability in climate models (Laepple and Huybers 2014; Laepple et al. 2023; Capotondi et al. 2023) or systematic bias on model response to historical anthropogenic forcings (Hwang et al. 2024; Kang et al. 2023; Kim et al. 2022).

Idealized experiments with coupled global climate models (CGCMs), in which the quadrupling of CO_2 (abrupt-4xCO2) is imposed on a control climate, are widely used to diagnose the climate feedback parameter. Using Green's function approach, Dong et al. (2020) found that the SST warming pattern cannot explain the intermodel difference in the climate feedback parameter in both CMIP5 and CMIP6 but can explain the intermodel difference in the climate feedback change in CMIP5. However, it is known that the results of Green's function are sensitive to the hyperparameters during its construction, like patch size, perturbation amplitude, and the AGCM used (Bloch-Johnson et al. 2024; Zhang et al. 2023). To accurately diagnose the factors that contribute to the intermodel spread of climate feedback, we design, perform, and analyze a series of sensitivity experiments. Our aim is to separate and quantify the contributions from the AGCM and SST to the intermodel differences in the climate feedback parameter. We find that the differences in SST, both warming pattern and climatology, have an insignificant impact in the intermodel spread of the climate feedback parameter and cloud feedback in the latest CMIP6 (Eyring et al. 2016). In contrast, the differences in AGCM (model physics) have a predominant influence of discrepancies in the climate model.

2. Data and methods

a. *AGCMs used: HiRAM, AM2.5, and AM4*

Three AGCMs developed at NOAA's Geophysical Fluid Dynamics Laboratory (GFDL), HiRAM (Zhao et al. 2009), AM2.5 (Delworth et al. 2012), and AM4 (Zhao et al. 2018a,b) are used to perform the prescribed SST experiments. Two legacy models have not only higher, TC-permitting, horizontal resolution but also very different climate feedbacks/sensitivities:

TABLE 1. The AMIP models used in this study and their climate feedback parameter λ measured in amip-p4K experiments. The λ of HiRAM, AM2.5, and AM4 is calculated using the uniform 4K warming experiment.

Model	λ (W m^{-2} K^{-1})
BCC-CSM2-MR	−1.59
CESM2	−1.62
CNRM-CM6-1	−1.24
E3SM-1-0	−1.44
GFDL-CM4	−1.62
GISS-E2-1-G	−1.74
IPSL-CM6A-LR	−1.18
MIROC6	−1.77
MRI-ESM2-0	−1.62
TaiESM1	−1.54
HIRAM	−1.07
AM2.5	−1.94
AM4	−1.64

HiRAM has less negative λ [high effective climate sensitivity (ECS)] and AM2.5 has more negative λ (low ECS). The most germane differences between the HiRAM and AM2.5 model are in the convection and cloud parameterization schemes. Both models use the finite-volume dynamic core on the cubed-sphere grid with 50 km × 50 km horizontal resolution and 32 vertical levels. The third model, ~100 km × 100 km horizontal resolution version of AM4, is the latest generation atmospheric climate model at GFDL and participated in the CMIP6. We choose these three atmospheric models to cover the range of climate feedback parameter space of CMIP6 AGCMs (see Table 1). This strategic selection enhances the robustness of our findings.

We first perform uniform plus 2K and 4K warming (p2K and p4K) experiments (30 years) to diagnose the climate feedback parameter of HiRAM, AM2.5, and AM4. The warming is prescribed on the top of control SST, which is the monthly mean in 1986–2005 of PCMDI SST reconstructions based on observation (Hurrell et al. 2008). Sea ice coverage has a seasonal cycle but otherwise does not change over time and is the same for all experiments [1986–2005 mean of PCMDI sea ice coverage data (Hurrell et al. 2008)]. The total climate feedback parameter is derived by dividing the global-mean top of the atmosphere (TOA) radiative imbalance by the global-mean surface air temperature change in these uniform warming experiments (Table 1). We use the radiative kernel method to decompose the Planck, lapse rate, water vapor, albedo, and cloud feedback (Soden et al. 2008).

To validate the models' ability to accurately replicate the SST pattern effect, we also run a historical SST simulation with the fixed preindustrial forcing experiment. The SST data are PCMDI SST reconstructions, which are used for the standard CMIP6 AMIP experiment. With the fixed forcing, we diagnose λ by regressing the TOA radiative response onto the surface temperature change in a 30-yr moving window following Andrews et al. (2022). The time series of λ represent the temporal evolution of the climate feedback.

TABLE 2. The summary of the three decomposition experiments. The experiments are targeted to isolate the terms in Eq. (1) one by one and quantitatively assess their contribution to the intermodel spread of climate feedback parameters.

	Experiment target	Control	Perturbation
EXP1	The warming pattern from different CMIP6 models, ΔSST	HiRAM/AM2.5/AM4 run with observational SST climatology	HiRAM/AM2.5/AM4 run with control SST + ΔSST_i
EXP2	The climatological SST of different CMIP6 models, SSTclim, and ΔSST	HiRAM run with $SSTclim_i$	HiRAM run with $SSTclim_i$ + ΔSST_i
EXP3	The differences in the atmosphere model, AGCM	AMIP experiment in CMIP6	amip-p4K experiment in CMIP6

b. *Decomposition experiment design*

As we mentioned in the introduction, both the SST and the AGCM can modulate λ in the coupled simulations. A linear decomposition of the TOA radiation response indicates that we can future isolate the SST factor into warming pattern (ΔSST) and SST climatology (SSTclim) (appendix). So, we evaluate the source of the intermodel spread of the climate feedback parameter ($\Delta\lambda$) and quantify the contribution from three discernible factors, as outlined in Eq. (1):

$$\Delta\lambda = \Delta\lambda_{\text{SSTclim}} + \Delta\lambda_{\Delta\text{SST}} + \Delta\lambda_{\text{AGCM}} + \epsilon. \quad (1)$$

The meaning of the error term ϵ is discussed in the appendix and the conclusion.

We design a series of perturbation experiments to accurately quantify the role of the SST warming pattern (ΔSST) and SSTclim (EXP1 and EXP2 in Table 2). In addition, we take advantage of the amip-p4K experiment done within the CMIP6 protocol that allows us to explore the impact of different AGCMs more explicitly (EXP3 in Table 2). The detailed description can be found in the following subsection.

1) DIFFERENT SST WARMING PATTERN (EXP1)

To assess the role of ΔSST (warming pattern of SST), we take ΔSST_i from various models in CMIP6 (subscript "*i*" indicates the source model) to force the three AGCMs (HiRAM, AM2.5, and AM4). Nearly 10 CMIP6 models are chosen based on their climate sensitivity (sampled from low to high climate sensitivity/feedback, Table 3). The ΔSST_i are added on the top of the same control SST climatology (1871–90 mean of PCMDI SST). Sea ice coverage is fixed to preindustrial monthly climatology (1871–90 mean of PCMDI sea ice coverage). This reduces the albedo feedback since the sea ice is fixed and does not change with warming. Also, we keep the forcing at the preindustrial level. Compared with the coupled abrupt-4xCO_2 experiment, simulations with the same warming at a lower CO_2 concentration level tend to have slightly more negative longwave feedback because the atmosphere is more transparent (Qin et al. 2022; Good et al. 2012; Ingram 2010).

The whole time series (150 years) of ΔSST_i in the abrupt-4xCO2 experiment is used to produce a time series of radiative response in HiRAM/AM2.5/AM4, so we can further investigate the temporal change of the climate feedback parameter. To reduce the computational cost, we concatenate the first 25-yr ΔSST_i with another 25-yr ΔSST, which is the 5-yr average ΔSST_i starting from year 26 to year 150. This strategy accelerates the slow warming period, and we only need to run 50 years in total for each ΔSST_i. For clarity, we still refer to it as a 150-yr run. To estimate the error induced by the simulation acceleration strategy, we repeat the AM4 simulations with full 150-yr SST warming pattern from the CMIP6 abrupt-4xCO2 experiment. We find the results of the full 150-yr simulations do not change our conclusion, and further discussion is included in the results and supplementary. When comparing it with the corresponding simulation in CMIP6, we apply the same averaging method for CMIP6 data to insure an apples-to-apples comparison. The λ and λ_{cloud} are estimated by regression the annual mean TOA radiative response to the global-mean surface temperature (GMST) change using all simulation years. The same methods are also applied to EXP2.

2) DIFFERENT SST CLIMATOLOGY (EXP2)

In EXP2, we investigate the impact of SSTclim together with ΔSST. We run HiRAM with the SSTclim ($SSTclim_i$) from the piControl in CMIP6 as the control experiment. In the perturbation experiment, HiRAM is forced with the absolute SSTs taken from abrupt-4xCO2 experiments (equivalent to ΔSST_i on the top of the corresponding SSTclim, $SSTclim_i$). With the control and perturbation experiment, we can evaluate the extent to which the SST climatology and SST warming pattern is able to explain the intermodel difference in λ in the current generation of coupled models. Due to high computational cost, we only conduct 6 pairs of experiment.

TABLE 3. The coupled models that are selected to provide SSTs of their abrupt-4xCO2 experiment. The ECS and their climate feedback parameter λ are also listed. Both the ECS and λ are computed using the Gregory method (Gregory et al. 2004).

Model	ECS (K)	λ (W m^{-2} K^{-1})
ACCESS-CM2	4.7	−0.71
CANESM5	5.6	−0.66
CESM2	5.2	−0.65
CNRM-CM6-1	4.9	−0.73
GFDL-CM4	3.9	−0.82
GFDL-ESM4	2.7	−1.30
INM-CM4-8	1.8	−1.52
MIROC-ES2L	2.7	−1.54
MRI-ESM2-0	3.1	−1.08
NORESM2-LM	2.6	−1.33

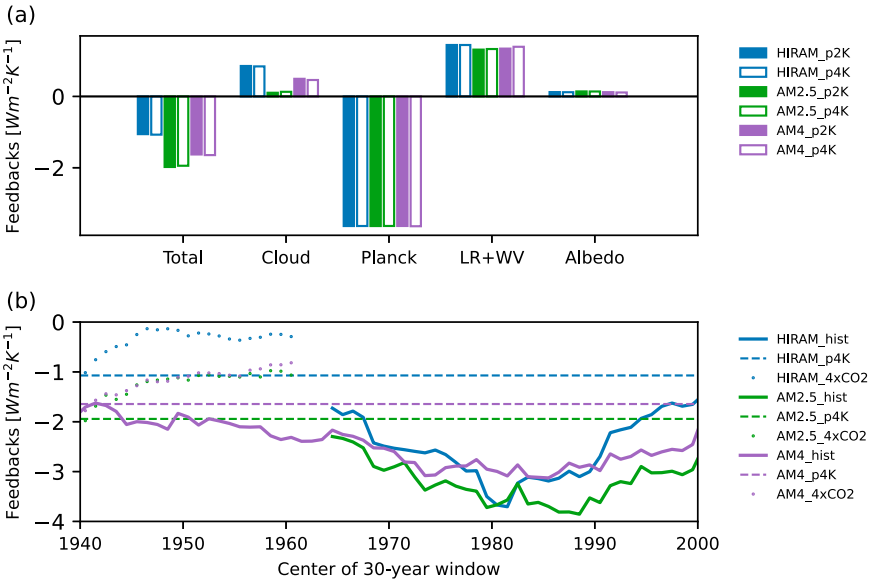

FIG. 1. Climate feedback parameter of HiRAM, AM2.5, and AM4. (a) The global surface temperature climate feedback parameters from the uniform warming experiments based on radiative feedback kernels of Soden et al. (2008). (b) The time-varying historical global surface temperature climate feedback parameter. Solid lines represent the time series of the climate feedback parameter in simulations only forced with historical SST. The model start year of AM4 is earlier than HiRAM and AM2.5. The dotted lines show λ of models forced with the SST warming pattern of the GFDL-CM4 model in the abrupt-4xCO2 experiment. They are part of EXP1.

3) DIFFERENT AGCMS: AMIP-P4K EXPERIMENTS (EXP3)

The amip-p4K is one of the experiments in the Cloud Feedback Model Intercomparison Project (CFMIP) (Webb et al. 2017) and can be used to diagnose the model dependence of the climate feedback parameter. In this experiment, different AGCMs are forced with the identical SST: a uniform 4K warming added to the observed SST from 1979 to 2014 period. We use its control experiment, the standard amip in CMIP6, to compute the TOA radiation and surface temperature change. Then, λ is derived by dividing the global-mean TOA radiative response by the global-mean surface air temperature change. Since there is only a trivial warming pattern in the uniform warming experiment, this definition is consistent with the conventional regression method (if we force the intercept to be zero). In EXP3, the difference in λ can be solely attributed to the difference in the atmosphere model itself.

3. The climate feedback parameter of HiRAM, AM2.5, and AM4

Before we explore the sensitivity experiments, we first examine the model dependence of the climate feedback parameter and the SST pattern effect across the three AGCMs. One way to evaluate λ for an atmospheric model (without a coupled ocean) is by performing uniform warming experiment (Cess and Potter 1988). In both the uniform 2K and 4K SST warming experiments, HiRAM shows less negative λ than AM2.5, while AM4 is in-between (Fig. 1a, Table 1). Decomposing the total climate feedback parameter using the radiative kernel method, we pinpoint that the difference mainly lies in the cloud feedback, which is supposed to be induced primarily by the different parameterizations across the three AGCMs.

While λ is similar in the uniform 2K and 4K warming experiment, λ derived from the historical SST-forced experiments shows substantial variation in the past few decades (solid lines in Fig. 1b). All models show more negative λ than the uniform SST warming scenarios and illustrate a strong historical pattern effect. In the limited sample size of three models, we see that the historical SST warming pattern caused λ to decrease before the 1980s and bounce back after the 1980s. Figure 2a shows that all three GFDL AGCMs have a larger warming rate in in Indo-Pacific warm pool (WP) region (15°N–15°S, 70°–150°E) than the global-mean warming around 1980 and then reduce after 1990. The warming in the WP region has nonlocal effect due the weak temperature gradient in the tropics and leads to more effective modification of the TOA flux than other regions.

The change of the climate feedback is dominated by the cloud feedback change since the clear-sky feedback shows much smaller variation over time than the all-sky feedback (Figs. 2b,c). However, three AGCMs adjust the feedback through different mechanisms. HiRAM shows a strong longwave feedback change (Fig. 2b) while AM2.5 shows a strong shortwave feedback change (Fig. 2c). The AM4 presents a combination of the modest longwave and shortwave feedback change. This difference is caused by the different cloud response to the same SST warming pattern in three models. Figure 2d shows the high-and low-cloud amount change per kelvin of

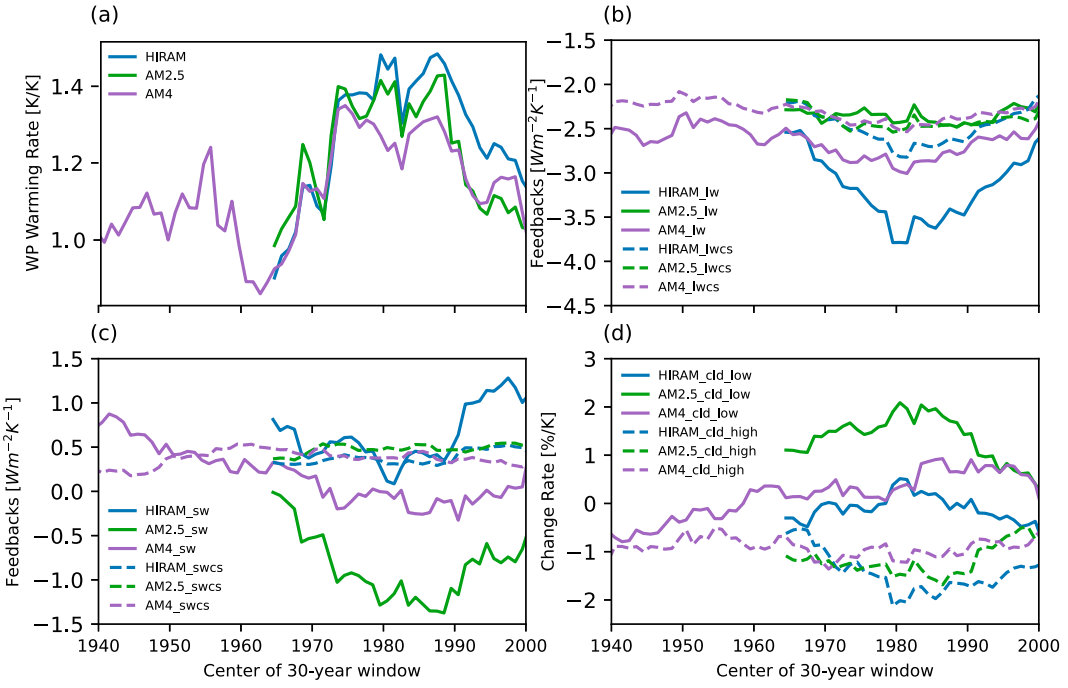

FIG. 2. (a) The warming in Indo-Pacific WP (15°N–15°S, 70°–150°E) per kelvin of GMST change. (b) Longwave and (c) shortwave climate feedback parameters in the clear-sky condition (dashed lines) and all-sky condition (solid lines). (d) The low- and high-cloud coverage change per K global-mean warming over time. Both the feedbacks and warming rates are computed using 30-yr data as in Fig. 1b.

global-mean warming. AM2.5 shows the largest low-cloud increase rate around 1980s which favors more shortwave reflection and leads to a strong negative shortwave climate feedback. HiRAM shows the largest high-cloud reduction rate around 1980s which leads to a more transparent atmosphere for outgoing longwave radiation and a more negative longwave climate feedback.

Although the historical SST pattern leads to a more negative λ, it does not simply scale with the model λ diagnosed in the uniform warming experiment. In Fig. 1b, AM4 has moderate λ and stays between HiRAM and AM2.5, but it has less negative λ than the other two models around 1980. This is first due to the smaller WP warming rate in AM4 than HiRAM and AM2.5 (Fig. 2a). Also, AM4 has smaller cloud responses in this period (Fig. 2d). It is also shown in Andrews et al. (2022) that different models could have a different amplitude of the pattern effect.

When we force the models with the SST taken from the coupled run of the idealized abrupt-4xCO2 experiment (here, we show the one from GFDL-CM4), λ increases over time (less negative, dotted lines in Fig. 1b). As we mentioned in the introduction, there have been many studies addressing the SST warming pattern in the historical period and idealized CO_2 forcing experiments and how it causes the opposite λ changes over time. In summary, idealized CO_2-forced experiments produce more warming in the eastern equatorial Pacific, while the recent historical warming presents more warming in the western equatorial Pacific. The warming in the western equatorial Pacific can cause a significant reduction in λ (more negative) by decreasing the magnitude of the cloud feedback (Dong et al. 2019; Andrews et al. 2018).

By examining the uniform warming and historical SST-forced simulations, we find that the three AGCMs have a wide range of λ and are able to produce SST pattern effect. We use them to further investigate the role of SST in the intermodel differences in λ in CMIP6 coupled models.

4. Evaluating CO_2-induced SST pattern effect via decomposition experiments

In this section, we analyze and quantify the contributions of ΔSST, SSTclim, and AGCM to the intermodel spread in climate feedback parameter and cloud feedback in CMIP6. We run two sets of prescribed SST experiments to assess ΔSST and SSTclim (EXP1 and EXP2) and use the amip-p4k experiment from CMIP6 to test AGCM (EXP3), as summarized in Table 2. A linear decomposition is also derived to formalize the question in the appendix.

a. The SST warming pattern (EXP1)

To quantify the role of the SST warming pattern (ΔSST), we take ΔSSTs from 10 models in CMIP6 abrupt-4xCO2 experiment, add it on the top of the same SST climatology, and force the three AGCMs. Then, we compute λ in three AGCMs and compare them with λ in the corresponding CMIP6 model. Figure 3 shows λ in HiRAM/AM2.5/AM4 versus λ in CMIP6. If the SST warming pattern is the only dominant factor that determines climate feedback parameter or cloud feedback, then we

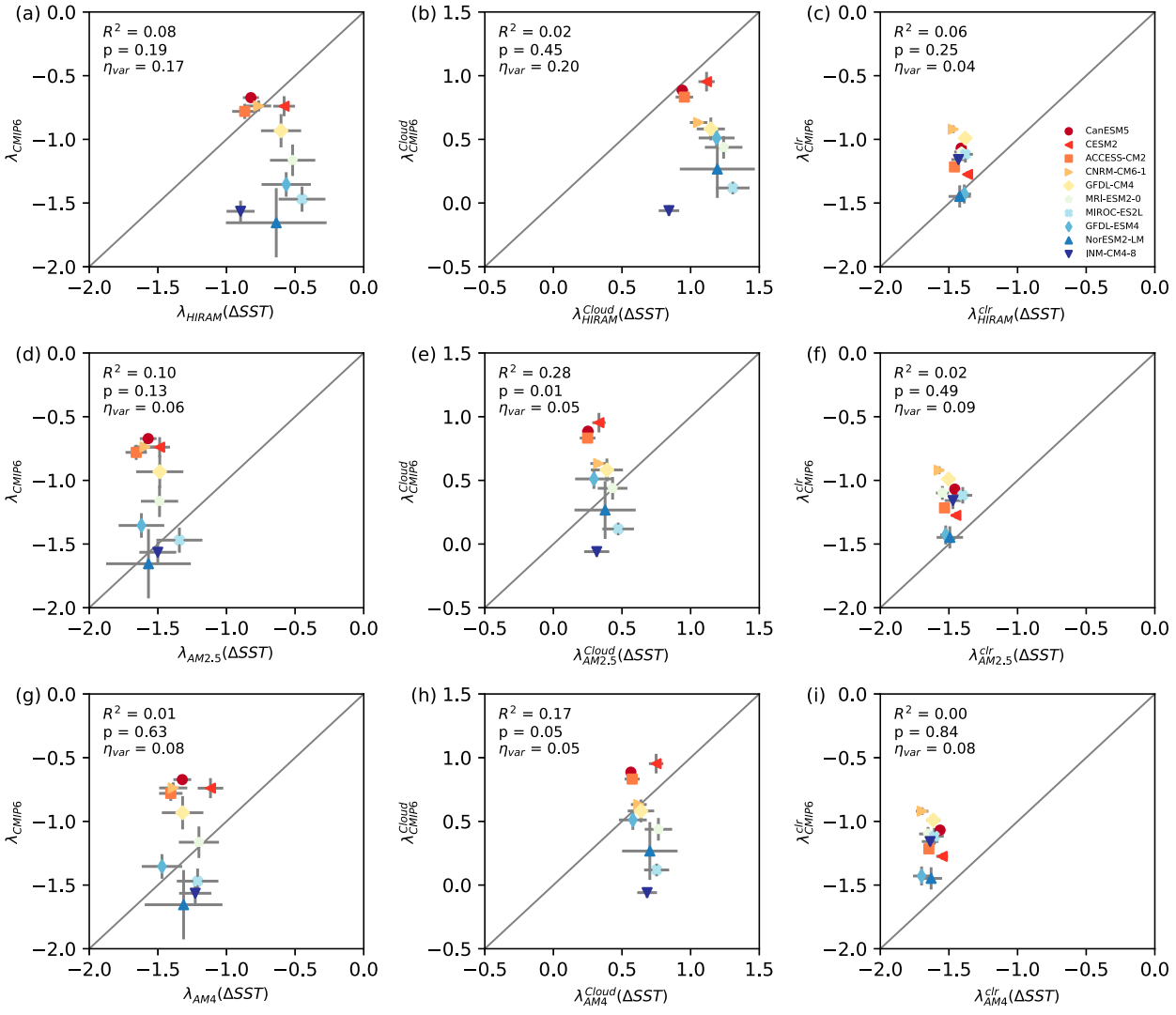

FIG. 3. Comparing the feedback in HiRAM/AM2.5/AM4 forced with warming patterns from 10 CMIP6 models and its corresponding 4xCO2 runs in CMIP6. (a),(d), (g) The total climate feedback parameter. (b),(e),(h) The cloud feedback. (c),(f),(i) The climate feedback parameter in the clear-sky condition. Each model is represented by a different mark as shown in the legend. The color of the markers represents the value of the total climate feedback in abrupt-4xCO_2 experiment, and red (blue) means more (less) positive. The black line shows the 1:1 line. The error bar on the marker indicates the uncertainty of the feedback (two standard deviations of the slope of the linear regression). The R^2 and p value of linear regression are shown in each plot. The ratio of the variance of x to y is noted as η_{var}.

should see the markers on the 1:1 line, since HiRAM/AM2.5/AM4 is experiencing the same ΔSST evolutions as the corresponding CMIP6 models.

The results indicate that ΔSST is not able to explain the intermodel difference in λ. In Fig. 3a, the markers are not on the 1:1 line and even do not show any statistically significant linear relationship between λ in CGCM and its corresponding SST runs using HiRAM (R^2 = 0.08). We also use radiative kernels to diagnose the cloud feedback. Figure 3b shows that the SST warming pattern also cannot predict the cloud feedback differences among models (R^2 = 0.02). Similar results are found with AM2.5 (Figs. 3d,e) and AM4 (Figs. 3g,h).

Beside the cloud feedback, there is also a noticeable spread in the clear-sky feedback among different models in CMIP6 and the three models used in this study (Figs. 3c,f,i). For these 10 CMIP6 models, the intermodel spread of the clear-sky feedback is dominated by the shortwave feedback, specifically the clear-sky albedo feedback (Fig. S1 in the online supplemental material). Since sea ice coverage is fixed in the AGCM simulations and the ice–albedo feedback is muted, it is not expected that AGCM simulations can reproduce the coupled model spread in shortwave clear-sky feedback. The AGCM simulations also fail to capture the clear-sky longwave feedback since they cannot reproduce the tropical free troposphere temperature warming and relative humidity change (Fig. S2). It indicates that the intermodel spread of the response of the large-scale atmosphere structure to warming is likely controlled by the atmosphere model difference instead of the warming pattern.

Based on the value of R^2, the total and cloud feedbacks are pretty much the same for different SST warming patterns with a small amount of explained variance compared to the CMIP6 range. Besides the linear correlation, we can evaluate the SST pattern effect using the ratio of variance in λ caused byΔSST to CMIP6 range, η_{var}. As noted in Fig. 3, η_{var} for the cloud feedback or total climate feedback parameter is less than 20% for HiRAM and less than 10% for AM2.5 and AM4. For simplicity, we average over the results from three AGCMs and two indices (R^2 and η_{var}) and summarize that the SST pattern effect explains the ~10% of the variance in total and cloud feedbacks among 10 coupled CMIP6 models. This result is in general consistent with Dong et al. (2020) in which Green's function is used to estimate the SST pattern effect on the climate feedback parameter in the first 20 years of the abrupt-4xCO_2 experiment ($\lambda_{1–20}$). Dong et al. (2020) found no correlation between the coupled model $\lambda_{1–20}$ and Green's function reconstructed $\lambda_{1–20}$ in both CMIP5 and CMIP6. Here, we compute λ using year 1–150, but the results remain the same for $\lambda_{1–20}$ that the SST pattern effect explains less than 10% of the coupled model variance in climate feedback (not shown). We repeat the same analysis with AM4 forced with full 150-yr SST warming patterns to ensure that the accelerated warming simulation do not alter our results. We find that the accelerated warming simulations do introduce <10% errors in estimated climate feedback parameters but do not affect the conclusion that the SST warming pattern does not explain the intermodel spread in climate feedback parameters in abrupt-4xCO_2 experiment (Fig. S3 and Table S1).

In contrast to λ, the SST pattern effect plays an important role in the climate feedback change $\Delta\lambda$. Here, $\Delta\lambda$ is defined as the difference between the climate feedback in year 25–150 to year 1–25. All three AGCMs forced with the coupled model SST warming pattern can capture the CMIP6 model climate feedback change $\Delta\lambda$ with a statistically significant correlation ($R^2 \approx 0.5$ in HiRAM and AM4, $R^2 \approx 0.3$ in AM2.5), shown by Fig. 4. It indicates that the different SST warming pattern in CIMP6 models contributes the intermodel spread of $\Delta\lambda$. Similar relationship is also found for the cloud feedback change ($\Delta\lambda^{Cloud}$) with smaller correlation (Figs. 4b,d,f). Dong et al. (2020) found that the evolving SST warming pattern is the key to understand the intermodel spread of $\Delta\lambda$ in CMIP5 but failed to capture the CMIP6 model $\Delta\lambda$ using Green's function approach. We speculate that the error introduced in Green's function method makes it not suitable to analyze the CMIP6 model $\Delta\lambda$.

b. *Impact of differences in SST climatology (EXP2)*

Besides the SST warming pattern, the climatological SST might also be relevant for climate feedback as shown in the linear decomposition in the appendix. Deep convection in tropics may alter the free-tropospheric temperature which set its threshold in both local and nonlocal regions due to weak temperature gradient (Sud et al. 1999; Johnson and Xie 2010; Zhang and Fueglistaler 2020; Williams et al. 2023). Differences in the SST climatology regulate the response of convection and cloud distributions even for the same SST warming pattern. For example, an El Niño–like background state may reduce the surface warming anomaly required to trigger the convection in central/eastern equatorial Pacific. On the other hand, a La Niña–like background state requires more surface warming anomaly to generate deep convection in this region. Hence, we include the SSTclim into our analysis to investigate its impact on the cloud and climate feedback.

In EXP2, we use the absolute SST ($SSTclim_i + \Delta SST_i$) instead of only the warming pattern (ΔSST_i + control SST) to force the HiRAM. With six control runs (with $SSTclim_i$), we can compute the climate feedback parameter and cloud feedback. In this way, we evaluate the impact of SSTclim and ΔSST together. Figure 5a shows λ of HiRAM forced by the absolute SST from CMIP6 models versus λ in the corresponding abrupt-4xCO_2 runs in CMIP6. We find that taking into account of the difference in SST climatology also does not improve the correlation between feedback in prescribed SST experiments and coupled model runs ($R^2 = 0.09$ vs $R^2 = 0.08$, $\eta_{var} = 0.05$ vs $\eta_{var} = 0.17$). The change in cloud feedback is almost indistinguishable with or without the SSTclim (Fig. 5b and Fig. S4). This set of experiment dismisses the hypothesis that the difference in SST climatology contributes to the intermodel difference in climate feedback in abrupt-4xCO2 experiment.

c. *Impact of difference in the atmospheric model (EXP3)*

The last factor is the AGCM. The amip-p4K experiment in CFMIP and its control amip experiment in CMIP6 are perfect to test the role of the atmosphere-only model. In amip-p4K experiment, all models are forced with the same SST warming and we can compute the feedbacks with the control–standard amip experiment. Figure 6a compares λ in coupled simulations and amip-p4K simulations. It shows a statistically significant linear correlation and indicates the differences in AGCM can explain more of the intermodel differences in the climate feedback parameter (45%) than in the pattern effect (10%). The predictability of cloud feedback in coupled simulation is higher [$(R^2 + \eta_{var})/2$%–50%, Fig. 6b] than the total climate feedback, which implies a strong influence of atmospheric physics on cloud feedback while the pattern effect is less effective (~10% in Fig. 3). In addition to the global mean climate feedback and cloud feedback, Qin et al. (2022) also showed that cloud property feedbacks and spatial distribution of cloud feedbacks in atmosphere-only and coupled models are highly correlated in both CMIP5 and CMIP6.

The offset in Fig. 6a is partially due to the albedo feedback being absent in amip-p4K, since the sea ice is the same as the control experiment. After subtracting the albedo feedback from total feedback in the abrupt-4xCO2 experiment, the offset is reduced (Fig. 6d) while R^2 and η_{var} are closed to unadjusted values.

More than half of the intermodel spread in the clear-sky feedback in the coupled models can be attributed to their atmospheric component (Fig. 6c). Specifically, the AGCM difference leads to different longwave clear-sky feedbacks as the correlation is higher after subtracting the clear-sky albedo feedback (Fig. 6e). This is because that the amip-p4K simulations can capture the coupled models' tropical free troposphere warming and relative

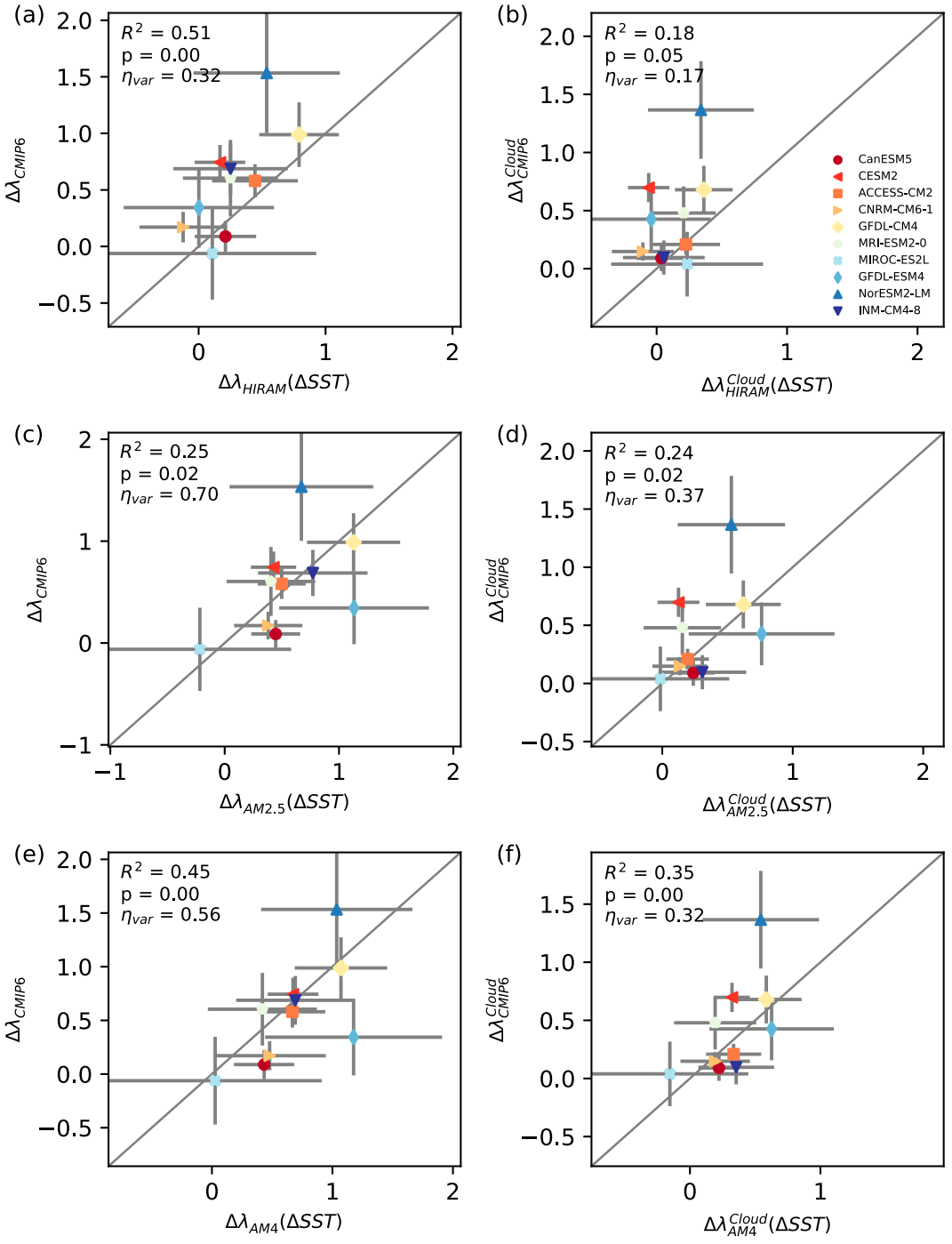

FIG. 4. As in Fig. 3, but for climate feedback change $\Delta\lambda$. The $\Delta\lambda$ is defined as the difference between the $\lambda_{25\text{–}150}$ and $\lambda_{1\text{–}25}$. (left) The change of the total climate feedback parameter ($\Delta\lambda$). (right) The change of the cloud feedback ($\Delta\lambda^{\text{Cloud}}$).

humidity change (Fig. S5), while the SST warming pattern–forced simulations cannot (Fig. S2). It indicates that the atmosphere model differences affect not only the cloud response to the warming but also the response of the large-scale atmosphere structure to the warming.

5. Conclusions and discussion

In this study, we quantify the extent to which SST, both the warming pattern and climatology, contributes to the intermodel spread in the climate feedback parameter and cloud feedback. By conducting a suite of prescribed SST experiment, we

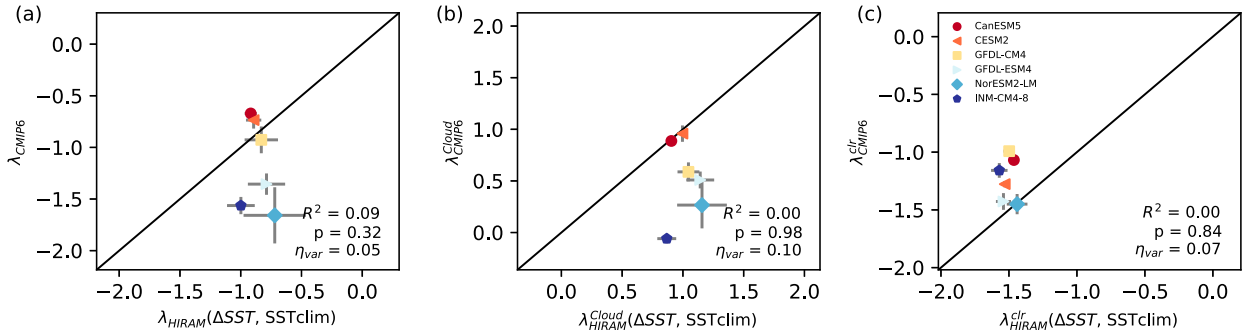

FIG. 5. Comparing the (a) total climate feedback, (b) cloud feedback, and (c) clear-sky feedback in HiRAM forced with absolute SST from 6 CMIP6 models and its corresponding abrupt-4xCO2 runs in CMIP6. The meaning of the marker and error bar is the same as in Fig. 3.

found that the SST differences do not account for the intermodel spread in climate feedback or the cloud feedback. In contrast, the atmospheric model differences can explain the coupled model behavior well. Our results highlight the prominent role of model physics, particularly the convection and cloud parameterizations, in determining cloud feedback and understanding model uncertainty of climate sensitivity.

a. *Temporal evolution of climate feedback and intermodel spread*

It is important to note that the intermodel spread in climate feedback is different from the time dependence of climate feedback (Armour et al. 2013; Dong et al. 2019; Andrews et al. 2015). HiRAM, AM2.5, and AM4 do exhibit time-varying climate feedback as shown in Fig. 1, and the decadal changes in feedback are generally consistent across these three models and with previously published results (Andrews et al. 2022). Meanwhile, HiRAM consistently generates a less negative climate feedback than AM2.5 in EXP1 (Fig. 3), which indicates that the differences in the atmospheric model impact the climate feedback and may dominate over the pattern effect difference across models in response to large abrupt CO_2 increases. We posit that observed historical changes in patterns of SST are more effective at modifying the feedback parameter than does

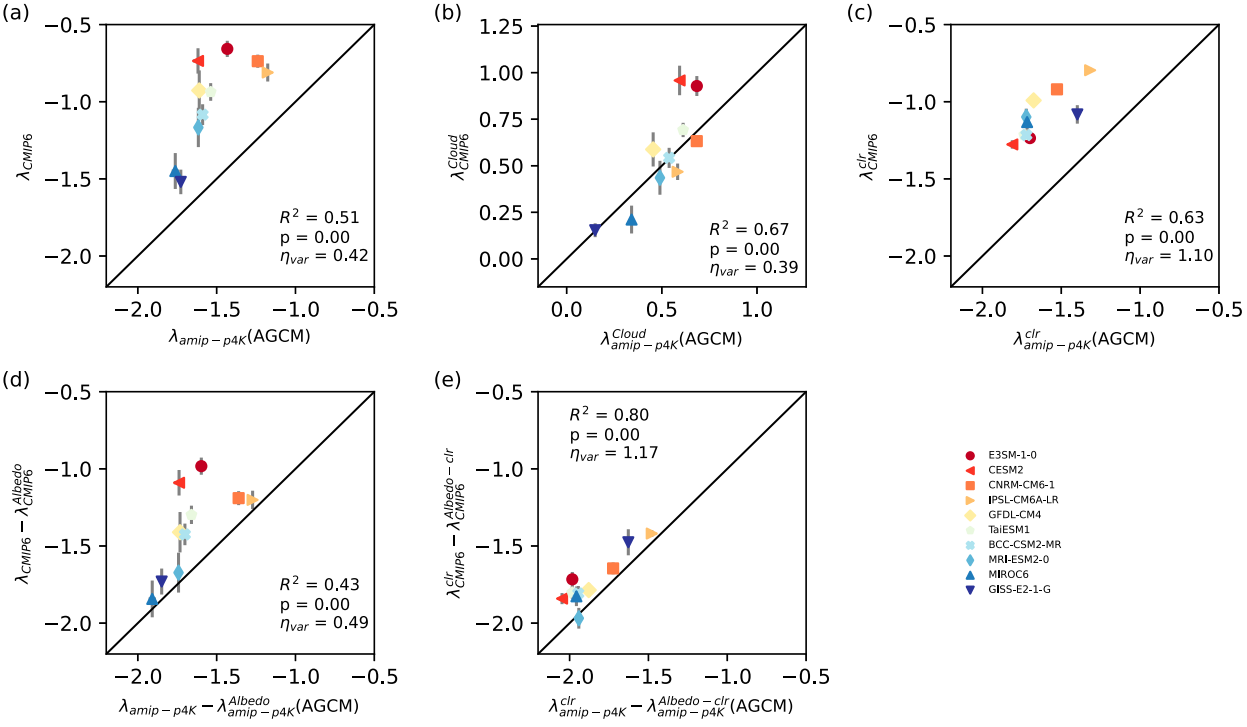

FIG. 6. (a) Climate feedback parameter, (b) cloud feedback, (c) clear-sky feedback, (d) nonalbedo feedback, and (e) clear-sky nonalbedo feedback in abrupt-4xCO2 and in amip-p4K experiment. The R^2 and p values of linear regression are shown in each plot. The ratio of the variance of x to y is noted as η_{var}. The color of the markers represents the value of feedback, and red (blue) means more (less) positive.

the intermodel spread in CO_2-induced SST response and SST climatology across the CMIP6 ensemble. It has been found that the reconstructed SST warming pattern over the past half century is peculiar compared to the historical SST warming patterns simulated by CGCMs, even accounting for difference model and large ensembles (Fueglistaler and Silvers 2021; Wills et al. 2022; Seager et al. 2022). It could suggest that climate models do not produce enough variability (Laepple and Huybers 2014; Laepple et al. 2023; Capotondi et al. 2023) or systematically biased on historical forcing and its response (Kang et al. 2023; Hwang et al. 2024; Kim et al. 2022).

b. *Nonlinear interaction between AGCM and SST*

Although we linearly decompose the intermodel difference in climate feedback into SST and AGCM factors, their impact on the climate feedback parameter of CGCM could be correlated. The results of previous sections show that the SST pattern effect leads to 10% of the intermodel difference in λ and AGCM differences contribute roughly 45% (50% for cloud feedback) in CMIP6. It indicates that a significant portion of intermodel spread is not explained (~45%, ~40% for cloud component), which indicates a strong nonlinear interaction between AGCM and SST.

The nonlinear interaction can present with different physical mechanisms. For example, one type of the SST warming pattern has a stronger impact on one AGCM than others. Different models respond differently for the same change as shown in the cloud controlling factor studies (e.g., Qu et al. 2015). A subset of CMIP6 models does show more positive shortwave cloud feedback in the Southern Ocean (Zelinka et al. 2020). Another possibility could be that one type of atmospheric physics parameterization (with high or low climate sensitivity) tends to generate a specific SST warming pattern. Previous studies also show that air–sea interaction can affect the SST warming pattern, like climatological latent heat flux (Xie et al. 2010) and hydrological change (Liu et al. 2021).

With around a few dozen data points (maybe less if we think of models from independent source), it might be hard to distinguish those possibilities by only analyzing the idealized coupled simulations. We advocate for more model centers to participate in the specialized experiments in CMIP6. Meanwhile, further understanding and theory on the formation of the SST warming pattern are also needed.

Acknowledgments. This work is supported by NOAA/MAPP Grant NA20OAR4310393 and the Carbon Mitigation Initiative at Princeton University. We acknowledge the World Climate Research Programme, which, through its Working Group on Coupled Modelling, coordinated and promoted CMIP5 and CMIP6. We also thank the climate modeling groups for producing and making available their model output, the Earth System Grid Federation (ESGF) for archiving the data and providing access, and the multiple funding agencies who support CMIP6 and ESGF.

Data availability statement. Source codes of three AGCMs used are all available online: 1) HiRAM (https://www.gfdl.noaa.gov/hiram-quickstart), 2) AM2.5 (https://www.gfdl.noaa.gov/cm2-5-and-flor-quickstart/), and 3) AM4 (https://www.gfdl.noaa.gov/coupled-physical-model-cm4/). CMIP6 data can be downloaded at https://esgf-node.llnl.gov/search/cmip6/. The simulation data can be accessed from the Zenodo repository: https://zenodo.org/doi/10.5281/zenodo.13760665.

APPENDIX

To the first order, the TOA radiative imbalance R is a function of SST for a given AGCM and forcing F. If we treat AGCM as a variable, then we can write

$$R = R(\text{SST}, \text{AGCM}, F).$$

Here, we assume that the land is dictated by the SST and does not change the first-order picture. Also, the role of sea ice coverage change is ignored. In all our simulations, sea ice is kept fixed. For both coupled or prescribed SST experiments, we can diagnose the radiative response ΔR due to the surface temperature change (excluding the forcing) as

$$\Delta R = R(\text{SST}_0 + \Delta\text{SST}, \text{AGCM}) - R(\text{SST}, \text{AGCM}),$$

where ΔSST is the warming pattern and SST represents the climatology (change to SSTclim hereafter). The climate feedback is the radiative response divided by the global-mean surface temperature change ΔT by definition:

$$\lambda = \Delta R/\Delta T.$$

Given ΔT is also a function of SSTclim, ΔSST, and AGCM *(if we think land response is part of AGCM)*, we can write the climate feedback as a function of SSTclim, ΔSST, and AGCM:

$$\lambda = \lambda(\text{SSTclim}, \Delta\text{SST}, \text{AGCM}). \tag{A1}$$

Therefore, we can attribute the intermodel spread of climate feedback into those three factors. In a simple linear framework,

$$\Delta\lambda = \frac{\partial\lambda}{\partial\text{SSTclim}}\Delta\text{SSTclim} + \frac{\partial\lambda}{\partial\Delta\text{SST}}\Delta(\Delta\text{SST}) + \frac{\partial\lambda}{\partial\text{AGCM}}\Delta\text{AGCM} + \epsilon, \tag{A2}$$

where ϵ represents the error of the above linear decomposition (nonlinear effect). The variables are abstract and symbolic; for example, the difference in AGCM cannot be represented by numbers (even if we assign a number, it does not have numerical meanings). Equation (1) is a simplified version of Eq. (A2).

If we fix two of three factors and only varying one factor, we can diagnose the contribution from the varying factor. For example, if we use one AGCM and add different warming patterns on the top of the same SSTclim, the difference in climate feedback represents how important the ΔSST is.

REFERENCES

Andrews, T., J. M. Gregory, M. J. Webb, and K. E. Taylor, 2012: Forcing, feedbacks and climate sensitivity in CMIP5 coupled

atmosphere-ocean climate models. *Geophys. Res. Lett.*, **39**, L09712, https://doi.org/10.1029/2012GL051607.

——, ——, and ——, 2015: The dependence of radiative forcing and feedback on evolving patterns of surface temperature change in climate models. *J. Climate*, **28**, 1630–1648, https://doi.org/10.1175/JCLI-D-14-00545.1.

——, and Coauthors, 2018: Accounting for changing temperature patterns increases historical estimates of climate sensitivity. *Geophys. Res. Lett.*, **45**, 8490–8499, https://doi.org/10.1029/2018GL078887.

——, and Coauthors, 2022: On the effect of historical SST patterns on radiative feedback. *J. Geophys. Res. Atmos.*, **127**, e2022JD036675, https://doi.org/10.1029/2022JD036675.

Armour, K. C., C. M. Bitz, and G. H. Roe, 2013: Time-varying climate sensitivity from regional feedbacks. *J. Climate*, **26**, 4518–4534, https://doi.org/10.1175/JCLI-D-12-00544.1.

Bjordal, J., T. Storelvmo, K. Alterskjær, and T. Carlsen, 2020: Equilibrium climate sensitivity above 5°C plausible due to state-dependent cloud feedback. *Nat. Geosci.*, **13**, 718–721, https://doi.org/10.1038/s41561-020-00649-1.

Bloch-Johnson, J., and Coauthors, 2024: The Green's Function Model Intercomparison Project (GFMIP) protocol. *J. Adv. Model. Earth Syst.*, **16**, e2023MS003700, https://doi.org/10.1029/2023MS003700.

Caldwell, P. M., M. D. Zelinka, K. E. Taylor, and K. Marvel, 2016: Quantifying the sources of intermodel spread in equilibrium climate sensitivity. *J. Climate*, **29**, 513–524, https://doi.org/10.1175/JCLI-D-15-0352.1.

——, ——, and S. A. Klein, 2018: Evaluating emergent constraints on equilibrium climate sensitivity. *J. Climate*, **31**, 3921–3942, https://doi.org/10.1175/JCLI-D-17-0631.1.

Capotondi, A., and Coauthors, 2023: Mechanisms of tropical Pacific decadal variability. *Nat. Rev. Earth Environ.*, **4**, 754–769, https://doi.org/10.1038/s43017-023-00486-x.

Ceppi, P., D. L. Hartmann, and M. J. Webb, 2016: Mechanisms of the negative shortwave cloud feedback in middle to high latitudes. *J. Climate*, **29**, 139–157, https://doi.org/10.1175/JCLI-D-15-0327.1.

Cess, R. D., and G. L. Potter, 1988: A methodology for understanding and intercomparing atmospheric climate feedback processes in general circulation models. *J. Geophys. Res.*, **93**, 8305–8314, https://doi.org/10.1029/JD093iD07p08305.

——, and Coauthors, 1990: Intercomparison and interpretation of climate feedback processes in 19 atmospheric general circulation models. *J. Geophys. Res.*, **95**, 16 601–16 615, https://doi.org/10.1029/JD095iD10p16601.

Delworth, T. L., and Coauthors, 2012: Simulated climate and climate change in the GFDL CM2.5 high-resolution coupled climate model. *J. Climate*, **25**, 2755–2781, https://doi.org/10.1175/JCLI-D-11-00316.1.

Dong, Y., C. Proistosescu, K. C. Armour, and D. S. Battisti, 2019: Attributing historical and future evolution of radiative feedbacks to regional warming patterns using a Green's function approach: The preeminence of the western Pacific. *J. Climate*, **32**, 5471–5491, https://doi.org/10.1175/JCLI-D-18-0843.1.

——, K. C. Armour, M. D. Zelinka, C. Proistosescu, D. S. Battisti, C. Zhou, and T. Andrews, 2020: Intermodel spread in the pattern effect and its contribution to climate sensitivity in CMIP5 and CMIP6 models. *J. Climate*, **33**, 7755–7775, https://doi.org/10.1175/JCLI-D-19-1011.1.

Eyring, V., S. Bony, G. A. Meehl, C. A. Senior, B. Stevens, R. J. Stouffer, and K. E. Taylor, 2016: Overview of the Coupled Model Intercomparison Project Phase 6 (CMIP6) experimental design and organization. *Geosci. Model Dev.*, **9**, 1937–1958, https://doi.org/10.5194/gmd-9-1937-2016.

Forster, P., and Coauthors, 2023: The Earth's energy budget, climate feedbacks and climate sensitivity. *Climate Change 2021: The Physical Science Basis*, V. Masson-Delmotte et al., Eds., Cambridge University Press, 923–1054.

Fueglistaler, S., and L. G. Silvers, 2021: The peculiar trajectory of global warming. *J. Geophys. Res. Atmos.*, **126**, e2020JD033629, https://doi.org/10.1029/2020JD033629.

Good, P., W. Ingram, F. H. Lambert, J. A. Lowe, J. M. Gregory, M. J. Webb, M. A. Ringer, and P. Wu, 2012: A step-response approach for predicting and understanding non-linear precipitation changes. *Climate Dyn.*, **39**, 2789–2803, https://doi.org/10.1007/s00382-012-1571-1.

Gregory, J. M., and Coauthors, 2004: A new method for diagnosing radiative forcing and climate sensitivity. *Geophys. Res. Lett.*, **31**, L03205, https://doi.org/10.1029/2003GL018747.

Hurrell, J. W., J. J. Hack, D. Shea, J. M. Caron, and J. Rosinski, 2008: A new sea surface temperature and sea ice boundary dataset for the Community Atmosphere Model. *J. Climate*, **21**, 5145–5153, https://doi.org/10.1175/2008JCLI2292.1.

Hwang, Y.-T., S.-P. Xie, P.-J. Chen, H.-Y. Tseng, and C. Deser, 2024: Contribution of anthropogenic aerosols to persistent La Niña-like conditions in the early 21st century. *Proc. Natl. Acad. Sci. USA*, **121**, e2315124121, https://doi.org/10.1073/pnas.2315124121.

Ingram, W., 2010: A very simple model for the water vapour feedback on climate change. *Quart. J. Roy. Meteor. Soc.*, **136**, 30–40, https://doi.org/10.1002/qj.546.

Johnson, N. C., and S.-P. Xie, 2010: Changes in the sea surface temperature threshold for tropical convection. *Nat. Geosci.*, **3**, 842–845, https://doi.org/10.1038/ngeo1008.

Kang, S. M., Y. Yu, C. Deser, X. Zhang, I.-S. Kang, S.-S. Lee, K. B. Rodgers, and P. Ceppi, 2023: Global impacts of recent Southern Ocean cooling. *Proc. Natl. Acad. Sci. USA*, **120**, e2300881120, https://doi.org/10.1073/pnas.2300881120.

Kim, H., S. M. Kang, J. E. Kay, and S.-P. Xie, 2022: Subtropical clouds key to Southern Ocean teleconnections to the tropical Pacific. *Proc. Natl. Acad. Sci. USA*, **119**, e2200514119, https://doi.org/10.1073/pnas.2200514119.

Laepple, T., and P. Huybers, 2014: Ocean surface temperature variability: Large model–data differences at decadal and longer periods. *Proc. Natl. Acad. Sci. USA*, **111**, 16 682–16 687, https://doi.org/10.1073/pnas.1412077111.

——, and Coauthors, 2023: Regional but not global temperature variability underestimated by climate models at supradecadal timescales. *Nat. Geosci.*, **16**, 958–966, https://doi.org/10.1038/s41561-023-01299-9.

Liu, M., G. Vecchi, B. Soden, W. Yang, and B. Zhang, 2021: Enhanced hydrological cycle increases ocean heat uptake and moderates transient climate change. *Nat. Climate Change*, **11**, 848–853, https://doi.org/10.1038/s41558-021-01152-0.

Manabe, S., and R. T. Wetherald, 1967: Thermal equilibrium of the atmosphere with a given distribution of relative humidity. *J. Atmos. Sci.*, **24**, 241–259, https://doi.org/10.1175/1520-0469(1967)024<0241:TEOTAW>2.0.CO;2.

McCoy, D. T., D. L. Hartmann, and D. P. Grosvenor, 2014: Observed Southern Ocean cloud properties and shortwave reflection. Part II: Phase changes and low cloud feedback. *J. Climate*, **27**, 8858–8868, https://doi.org/10.1175/JCLI-D-14-00288.1.

——, ——, M. D. Zelinka, P. Ceppi, and D. P. Grosvenor, 2015: Mixed-phase cloud physics and Southern Ocean cloud feedback

in climate models. *J. Geophys. Res. Atmos.*, **120**, 9539–9554, https://doi.org/10.1002/2015JD023603.

Mülmenstädt, J., and Coauthors, 2021: An underestimated negative cloud feedback from cloud lifetime changes. *Nat. Climate Change*, **11**, 508–513, https://doi.org/10.1038/s41558-021-01038-1.

Qin, Y., M. D. Zelinka, and S. A. Klein, 2022: On the correspondence between atmosphere-only and coupled simulations for radiative feedbacks and forcing from CO_2. *J. Geophys. Res. Atmos.*, **127**, e2021JD035460, https://doi.org/10.1029/2021JD035460.

Qu, X., A. Hall, S. A. Klein, and A. M. DeAngelis, 2015: Positive tropical marine low-cloud cover feedback inferred from cloud-controlling factors. *Geophys. Res. Lett.*, **42**, 7767–7775, https://doi.org/10.1002/2015GL065627.

Sanderson, B. M., C. Piani, W. J. Ingram, D. A. Stone, and M. R. Allen, 2008: Towards constraining climate sensitivity by linear analysis of feedback patterns in thousands of perturbed-physics GCM simulations. *Climate Dyn.*, **30**, 175–190, https://doi.org/10.1007/s00382-007-0280-7.

Seager, R., N. Henderson, and M. Cane, 2022: Persistent discrepancies between observed and modeled trends in the tropical Pacific Ocean. *J. Climate*, **35**, 4571–4584, https://doi.org/10.1175/JCLI-D-21-0648.1.

Sherwood, S. C., and Coauthors, 2020: An assessment of Earth's climate sensitivity using multiple lines of evidence. *Rev. Geophys.*, **58**, e2019RG000678, https://doi.org/10.1029/2019RG000678.

Soden, B. J., I. M. Held, R. Colman, K. M. Shell, J. T. Kiehl, and C. A. Shields, 2008: Quantifying climate feedbacks using radiative kernels. *J. Climate*, **21**, 3504–3520, https://doi.org/10.1175/2007JCLI2110.1.

Sud, Y. C., G. K. Walker, and K.-M. Lau, 1999: Mechanisms regulating sea-surface temperatures and deep convection in the tropics. *Geophys. Res. Lett.*, **26**, 1019–1022, https://doi.org/10.1029/1999GL900197.

Tan, I., T. Storelvmo, and M. D. Zelinka, 2016: Observational constraints on mixed-phase clouds imply higher climate sensitivity. *Science*, **352**, 224–227, https://doi.org/10.1126/science.aad5300.

Wang, C., B. J. Soden, W. Yang, and G. A. Vecchi, 2021: Compensation between cloud feedback and aerosol-cloud interaction in CMIP6 models. *Geophys. Res. Lett.*, **48**, e2020GL091024, https://doi.org/10.1029/2020GL091024.

Webb, M. J., and Coauthors, 2017: The Cloud Feedback Model Intercomparison Project (CFMIP) contribution to CMIP6. *Geosci. Model Dev.*, **10**, 359–384, https://doi.org/10.5194/gmd-10-359-2017.

Williams, A. I. L., N. Jeevanjee, and J. Bloch-Johnson, 2023: Circus tents, convective thresholds, and the non-linear climate response to tropical SSTs. *Geophys. Res. Lett.*, **50**, e2022GL101499, https://doi.org/10.1029/2022GL101499.

Wills, R. C. J., Y. Dong, C. Proistosecu, K. C. Armour, and D. S. Battisti, 2022: Systematic climate model biases in the large-scale patterns of recent sea-surface temperature and sea-level pressure change. *Geophys. Res. Lett.*, **49**, e2022GL100011, https://doi.org/10.1029/2022GL100011.

Winton, M., K. Takahashi, and I. M. Held, 2010: Importance of ocean heat uptake efficacy to transient climate change. *J. Climate*, **23**, 2333–2344, https://doi.org/10.1175/2009JCLI3139.1.

Xie, S.-P., C. Deser, G. A. Vecchi, J. Ma, H. Teng, and A. T. Wittenberg, 2010: Global warming pattern formation: Sea surface temperature and rainfall. *J. Climate*, **23**, 966–986, https://doi.org/10.1175/2009JCLI3329.1.

Zelinka, M. D., T. A. Myers, D. T. McCoy, S. Po-Chedley, P. M. Caldwell, P. Ceppi, S. A. Klein, and K. E. Taylor, 2020: Causes of higher climate sensitivity in CMIP6 models. *Geophys. Res. Lett.*, **47**, e2019GL085782, https://doi.org/10.1029/2019GL085782.

Zhang, B., M. Zhao, and Z. Tan, 2023: Using a Green's function approach to diagnose the pattern effect in GFDL AM4 and CM4. *J. Climate*, **36**, 1105–1124, https://doi.org/10.1175/JCLI-D-22-0024.1.

Zhang, Y., and S. Fueglistaler, 2020: How tropical convection couples high moist static energy over land and ocean. *Geophys. Res. Lett.*, **47**, e2019GL086387, https://doi.org/10.1029/2019GL086387.

Zhao, M., 2014: An investigation of the connections among convection, clouds, and climate sensitivity in a global climate model. *J. Climate*, **27**, 1845–1862, https://doi.org/10.1175/JCLI-D-13-00145.1.

——, I. M. Held, S.-J. Lin, and G. A. Vecchi, 2009: Simulations of global hurricane climatology, interannual variability, and response to global warming using a 50-km resolution GCM. *J. Climate*, **22**, 6653–6678, https://doi.org/10.1175/2009JCLI3049.1.

——, and Coauthors, 2016: Uncertainty in model climate sensitivity traced to representations of cumulus precipitation microphysics. *J. Climate*, **29**, 543–560, https://doi.org/10.1175/JCLI-D-15-0191.1.

——, and Coauthors, 2018a: The GFDL global atmosphere and land model AM4.0/LM4.0: 1. Simulation characteristics with prescribed SSTs. *J. Adv. Model. Earth Syst.*, **10**, 691–734, https://doi.org/10.1002/2017MS001208.

——, and Coauthors, 2018b: The GFDL global atmosphere and land model AM4.0/LM4.0: 2. Model description, sensitivity studies, and tuning strategies. *J. Adv. Model. Earth Syst.*, **10**, 735–769, https://doi.org/10.1002/2017MS001209.

Zhou, C., M. D. Zelinka, and S. A. Klein, 2016: Impact of decadal cloud variations on the Earth's energy budget. *Nat. Geosci.*, **9**, 871–874, https://doi.org/10.1038/ngeo2828.

——, ——, and ——, 2017: Analyzing the dependence of global cloud feedback on the spatial pattern of sea surface temperature change with a Green's function approach. *J. Adv. Model. Earth Syst.*, **9**, 2174–2189, https://doi.org/10.1002/2017MS001096.